Evaluation of Blood Flow in Pancreatic Ductal Carcinoma Using Contrast-Enhanced, Wide-Band Doppler Ultrasonography

Correlation With Tumor Characteristics and Vascular Endothelial Growth Factor

Tadashi Ohshima, MD, Taketo Yamaguchi, MD, Takeshi Ishihara, MD, Masaharu Yoshikawa, MD, Akitoshi Kobayashi, MD, Nobuyuki Sakaue, MD, Takeshi Baba, MD, Syuji Yamada, MD, and Hiromitsu Saisho, MD

Background and Aims: Tumor vascularization has been attracting attention. However, there have been only a few reports on tumor vascularization in pancreatic ductal carcinoma, especially on vascularization depicted by imaging modalities. We investigated the relationship among wide-band Doppler signals, clinicopathological factors, and vascular endothelial growth factor (VEGF) expression.

Methods: Sixty-nine patients with pancreatic ductal carcinoma were investigated. The vascular signals from carcinoma lesions were assessed by contrast-enhanced, wide-band Doppler ultrasonography (dynamic flow). VEGF expression was quantitated by enzyme immunoassay for 28 patients. Depending on the intensity of the signals, the patients were classified into type A (definite vascular signal) or type B (almost no vascular signal).

Results: Type A patients and type B patients accounted for 65% and 35% of patients, respectively. According to multivariate analysis of vascular signal type and clinicopathological factors, liver metastasis occurred significantly more frequently in the type A group. VEGF expression was also significantly higher in the type A group than in the type B group.

Conclusions: Dynamic flow has very high sensitivity for detecting the vascular signals from pancreatic ductal carcinoma. The quantity of vascular signals correlated with tumor characteristics and VEGF.

Key Words: pancreatic carcinoma, liver metastasis, Levovist, wide-band Doppler ultrasonography, vascular endothelial growth factor

(*Pancreas* 2004;28:335–343)

Received for publication March 21, 2003; accepted September 5, 2003.

From the Department of Medicine and Clinical Oncology (Drs Ohshima, Yamaguchi, Ishihara, Yoshikawa, Kobayashi, Sakaue, Baba, and Saisho), Graduate School of Medicine, Chiba University, Chiba, Japan; and the National Institute of Radiological Sciences (Dr Yamad), Chiba, Japan.

Reprints: Dr. Tadashi Ohshima, 1-8-1 Inohana, Chuuou-ku, Chiba-city, Chiba Prefecture, 2608670 Japan (e-mail: ohshima@ah.wakwak.com).

Recently, the relationship of tumor vascularization to qualitative diagnosis as well as to the treatment and prognosis of tumor has been attracting attention.[1–7] However, there have been only a few reports on tumor vascularization in pancreatic ductal carcinoma (PC).[4,7–11]

Since the development of Levovist as a signal intensifier for the color Doppler method,[12–16] tumor vascularization has come to be assessed by contrast-enhanced ultrasonography. The development of new techniques such as the second harmonic method that can indicate the blood flow in B mode,[17,18] the color Doppler method making use of the second harmonic method[19,20] and pulse inversion method[21–24] has made it possible to capture vascular flow at high resolution. It was, however, difficult to observe the intratumoral hemodynamic pattern in the pancreas with the conventional contrast Doppler method and even with the contrast harmonic method.

In the current study, we used a new contrast-enhanced ultrasonography technique[25] characterized by high sensitivity, high resolution, and low artifact to investigate the intratumoral vascular signal in PC lesions and to compare the results with those obtained by contrast-enhanced computed tomography (dynamic CT). We also investigated the presence and absence of correlation between intratumoral blood flow and clinicopathological factors. Furthermore, we quantitated vascular endothelial growth factor (VEGF), a major vascular growth factor, to investigate correlation between the intratumoral vascular signal by dynamic flow and the expression of VEGF in the tumor tissue.

PATIENTS AND METHODS

Patients

The subjects of this study were 69 patients with pancreatic ductal carcinoma [48 men and 21 women; mean age, 63.5 ± 8.5 years (range, 39–78)] who were diagnosed and treated at this hospital between September 2000 and December 2002. The mean tumor diameter was 3.7 ± 1.5 cm (range, 1.0–

7.0). The site of tumor was the head of the pancreas in 33 patients and the body or tail in the 36 patients. PC was diagnosed by resection in 33 cases, by transcutaneous needle biopsy specimen from the pancreatic lesion in 30 cases, cytodiagnosis of ascites in 5, and cytodiagnosis of pancreatic fluid in 1. According to TNM classification,[26,27] 7 were in stage I, 8 in stage II, 9 in stage III, and 45 in stage IV. For patients who did not undergo surgery, staging was done by dynamic CT and ultrasonographic endoscopy. Follow-up for all patients ranged from 9 to 958 days; the follow-up period ended on May 30, 2003. Forty-one patients died; the survival time ranged from 9 to 531 days. The median survival time was 200 days and the mean survival time was 201 ± 117 days. Forty-two patients survived and the survival time ranged from 96 to 958 days. The median survival time was 338 days and mean survival time was 351 ± 206 days. Informed consent was obtained from all patients before conducting contrast-enhanced ultrasonography and tissue collection for VEGF measurement.

Contrast-Enhanced, Wide-Band Doppler Ultrasonography

A Power Vision 8000 (Toshiba) was mounted on a wide-band dynamic flow for Doppler ultrasonography device. As a probe, a 3.75-MHz convex type was used. A contrast medium, Levovist (Schering, Berlin, Germany), was adjusted to 300 mg/mL, and a bolus intravenous injection of 8 mL into an antecubital vein was performed through a 22-gauge Teflon needle. The vascular signals from the tumor were continuously observed for 2 minutes immediately after administration. One focal point was established in the lower edge of tumor. The mechanical index, pulse repetition frequency, and frame rate using default were 0.8–1.4, 3.0–3.9 kHz, and 4–7 frames per seconds, respectively. Based on the image recorded on magnetooptical disk and S-VHS tape, the intensities of intratumoral vascular signals were classified into type A, whose signals were macroscopically discernible, and type B, whose signals were only minimally detectable. Two specialists in ultrasonography (T. O., T. Y.) were responsible for macroscopic classification. They were blind to information on tumors concerning the findings of dynamic CT and histology. Any inconsistency in findings was solved by discussion. As the next step, the frame showing the maximal contrast effect was selected from the recorded images, and the vascular signal area against the tumor area (signal ratio) was calculated using Photo Shop 4.0 (Adobe Systems Inc., CA) to evaluate the intratumoral vascular signal obtained by dynamic flow (Fig. 1).

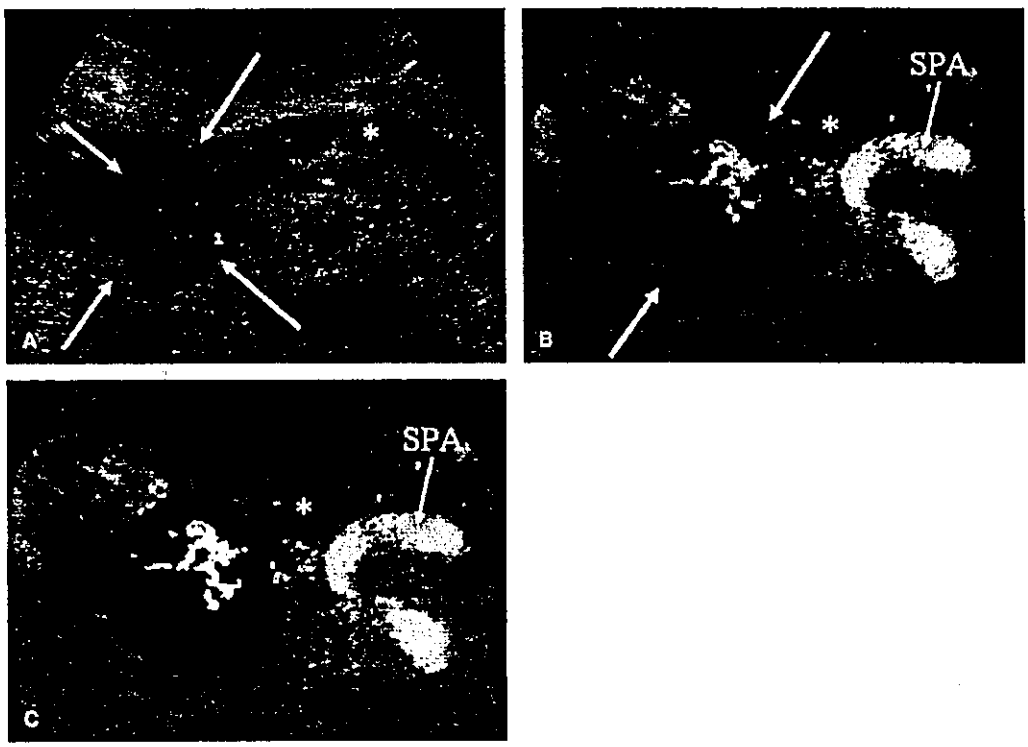

FIGURE 1. Calculation of vascular signal ratio in tumor. A: The ultrasonographic image before injection of contrast medium. Adenocarcinoma measuring 3.5 cm in the head is shown (diagnosed by a needle biopsy specimen from the pancreatic lesion). B: The image captured by dynamic flow 45 seconds after administration of contrast medium. Tortuous vessels are detected in the tumor. C: Vascular signals extracted in comparison with B and using Photo Shop's 2-level program. The signal ratio is calculated by a histogram program as the percentage of the tumor area highlighted by the signal. The signal ratio was 11.8% in this case.

Dynamic CT

A SOMATOM Plus 4 Somaris (Siemens) was used for dynamic CT. After injection of 150 mL of 300 mgI/ml contrast medium into an antecubital vein at a rate of 3 mL/s, the arterial, portal, and late phases were captured by a delay of 30, 80, and 180 seconds, respectively, with 5-mm collimation. The patient was diagnosed as having liver metastasis when an intrahepatic tumor lesion was detected by image diagnosis and adenocarcinoma was found on biopsy.

Quantitation of VEGF in Tissue

Tumor tissue samples were collected from 28 patients by resection or percutaneous needle biopsy from the pancreatic lesion under ultrasonographic guidance using a 21-gauge needle. Samples from nontumorous pancreatic tissue were also collected from 9 cases of resection. Tissue specimens were homogenized in 300 μL of PBS buffer. The centrifuged supernatant was used in the VEGF measurement by enzyme immunoassay (EIA). The same measurement kit used by Kido et al[28] was used in EIA. To the plate solidified with mouse monoclonal antibody for human $VEGF_{165}$, 50 μL of the above-mentioned supernatant was added. Then, rabbit anti-$hVEGF_{165}$ polyclonal antibody was added as the secondary antibody, after which HRP-labeled anti-rabbit IgG was added for colorimetric quantitation. The detection sensitivity was 20 pg/mL.

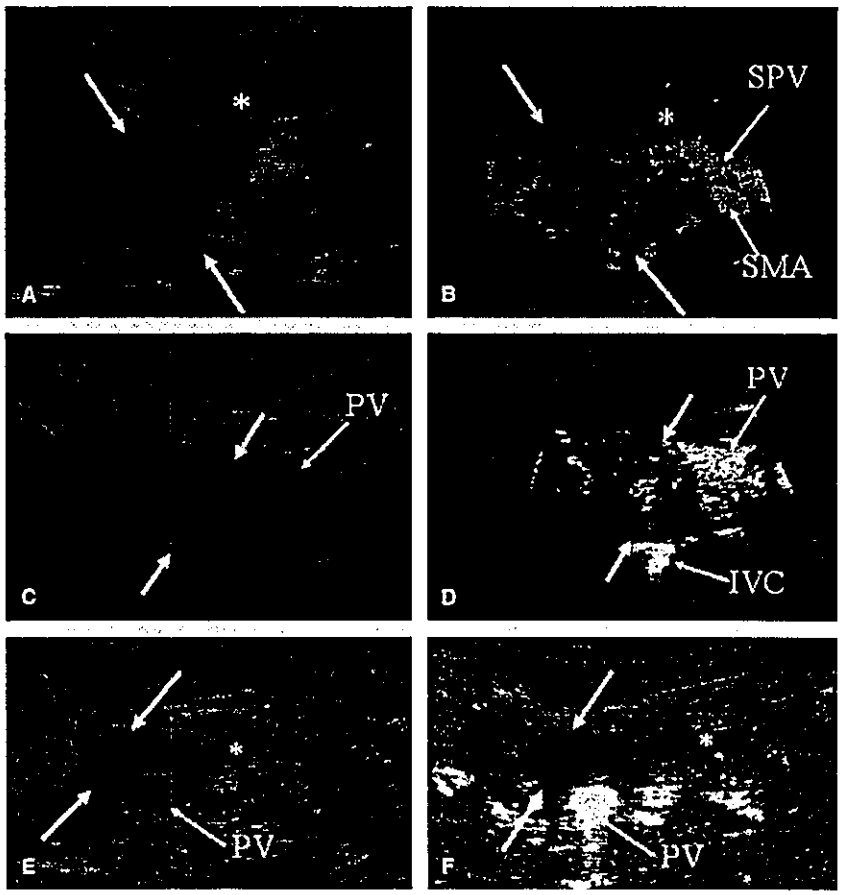

FIGURE 2. Type classification by intensity of intratumoral vascular signal. A: The ultrasonographic image before injection of the contrast medium. Well-differentiated ductal adenocarcinoma (bold arrow) measuring 4 cm in the head is shown. B: The image captured by dynamic flow 40 seconds after administration of the contrast medium. A strong vascular signal is observed in the tumor (bold arrow). This case is classified as type A. C: The ultrasonographic image before injection of the contrast medium. Poorly differentiated ductal adenocarcinoma (bold arrow) measuring 3 cm in the head is shown. D: The image captured by dynamic flow 35 seconds after administration of the contrast medium. Spotted vascular signals are observed in the intratumoral blood flow (bold arrow). This case is classified as type A. E: The ultrasonographic image before injection of the contrast medium. Moderately differentiated ductal adenocarcinoma (bold arrow) measuring 2 cm in the head is shown. f: The image captured by dynamic flow 40 seconds after administration of the contrast medium. Hardly any vascular signal is noted in the tumor (bold arrow). This case is classified as type B. PV, portal vein; SPV, splenic vein; SPA, splenic artery.

Statistical Analysis

The Mann-Whitney *U* test was used for comparison of continuous variables between the 2 groups. Single regression analysis was performed for comparison between the continuous variables. The Fisher exact test was employed for comparison of categorical variables between the 2 groups. The Kruskal-Wallis test was applied for comparison among 3 or more groups. The factors demonstrating a significant difference in the univariate analysis were assessed for their influence on the vascular signal type. For multivariate analysis, logistic regression analysis was used. Kaplan-Meier survival analysis was used to estimate the survival time, and log rank test was used to compare differences between 2 groups. Stat View version 5 (Abacus Concepts Inc., Berkeley, CA) was employed for the above statistical analyses. The differences with a probability of ≤5% were considered to be statistically significant ($P < 0.05$). The figures obtained were indicated in mean ± standard deviation (SD).

RESULTS

Assessment of Intratumoral Vascular Flow Detected by Dynamic Flow

According to the results obtained with dynamic flow, 45 patients (65%) were classified into type A, which demonstrated intratumoral vascular signal, while 24 patients (35%) were classified into type B, which demonstrated hardly any signal. Figure 2 shows typical examples. The vascular signal ratios from PC were 15.4% ± 8.6% (6.1%–44.3%) in type A patients and 2.1% ± 1.5% (0.2%–5.6%) in type B patients. Figure 3 shows the distribution of type A and type B vascular signal ratio. With the signal ratio of 6% as the borderline, the type A and type B vascular signal ratio corresponded with the results of macroscopic classification.

Comparison with Dynamic CT

The tumor was demonstrated in 65 patients (94%) as a low-density area in the arterial phase and portal phase. However, the tumor was not imaged in 4 cases (6%) due to isodensity. On dynamic CT, the tumor of 44 patients among the 45 in the type A group was imaged as a low-density area (Fig. 4).

Comparison of Intratumoral Vascular Signal with Clinicopathology

Comparison by Univariate Analysis (Table 1)

Tumor diameter

The diameters of tumors in the patients classified into type A and type B were 4.0 ± 1.5 cm (1.5–7 cm) and 3.2 ± 1.3 cm (1–7 cm), respectively, indicating a significant difference between the type A group and type B group ($P = 0.0233$).

Liver metastasis

Metastases to the liver occurred in 19 of the 45 type A patients. On the other hand, metastases were noted in only 2 of the 24 type B patients. There was a significant difference between the type A and B groups ($P = 0.0052$).

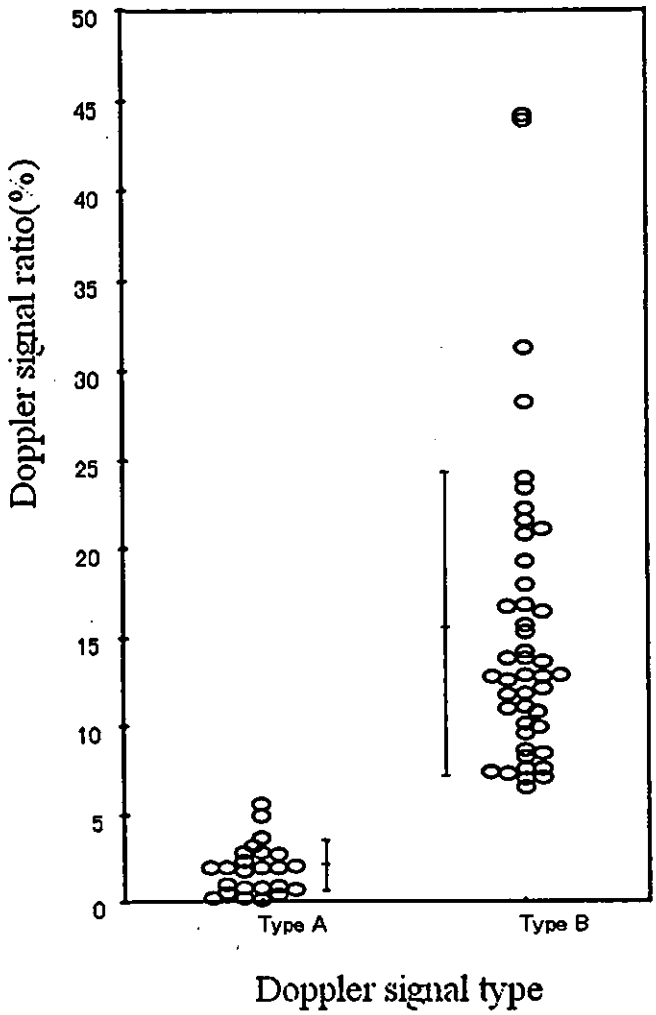

FIGURE 3. Relationship between the vascular signal type of pancreatic ductal carcinoma detected by dynamic flow and vascular signal ratio. The vascular signal ratios from pancreatic ductal carcinoma were 15.6 ± 8.7% (6.1%–44.3%) in type A patients and 1.9 ± 1.6% (0.2%–5.6%) in type B patients. The distribution of type A and type B vascular signal ratios is shown. With the signal ratio of 6% as the borderline, the type A and type B vascular signal ratios corresponded with the results of macroscopic classification. Circle, Each case; bar: mean ± SD.

TNM categories

T1-T2 and T3-T4 were 5 and 40 patients in type A and 9 and 15 patients in type B. Type A patients had a significantly higher T category than type B patients ($P = 0.0261$). Although there was no definite correlation between the intensity of intratumoral vascular signal and TNM stage, type A patients tended to be classified into advanced stage more frequently than type B patients ($P = 0.0696$).

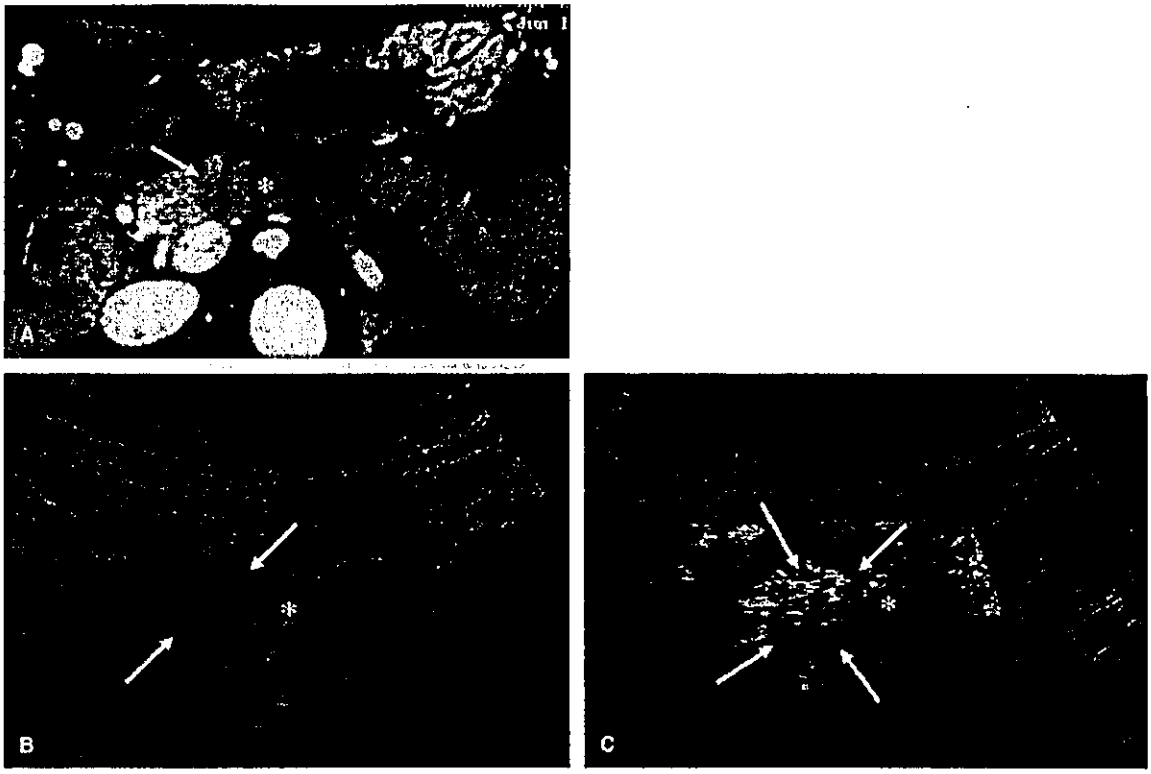

FIGURE 4. Case used for comparison with dynamic CT. This case had poorly differentiated ductal adenocarcinoma measuring 16 mm in the body. A: The arterial phase captured by dynamic CT. A low-density area (arrow) in the body and dilation (*) in the pancreatic duct in the tail are observed. B: The ultrasonographic image before injection of contrast medium. A hypoechoic tumor is observed in the body (arrow). C: The image captured by dynamic flow 35 seconds after administration of contrast medium. Vascular signals are observed in the tumor (arrow). The signal ratio was 13.9%. Asterisk, dilated main pancreatic duct in the tail.

Tumor differentiation

According to the results obtained from the 49 patients whose histologic grading of tumor was specifiable, there was no significant difference in histologic type of tumor between the type A and B groups ($P = 0.8180$).

Results of Multivariate Analysis (Table 2)

Intratumoral vascular signal type detected by dynamic flow demonstrated a significant correlation with liver metastasis ($P = 0.0435$), and the type A group exhibited tendency toward a higher T category ($P = 0.0886$).

Patient Prognosis

Survival time

The median survival time of type A patients was 218 days and that of type B patients was 284 days. The mean survival time of type A patients was 283 ± 115 days and that of type B patients was 349 ± 241 days. The mean survival of type A patients was significantly shorter than that of type B patients ($P = 0.0435$) (Fig. 5).

Liver metastasis

Hepatic metastases occurred in 6 of the 26 type A patients who had no hepatic metastases at the sonographic examination. Only one of the 22 type B patients developed liver metastases during the follow-up period.

Comparison of Amount of VEGF Expression and Clinicopathology (Table 3)

VEGF expression

The amount of VEGF expression in nontumorous sites was 408 ± 255 (46–483) ng/mg protein versus 1469 ± 1419 (226–3956) ng/mg protein in tumorous sites, indicating a significant difference between the 2 sites ($P = 0.0305$) (Fig. 6). The VEGF expression in the latter was 3.6 times that in the former on average.

Intratumoral vascular signal type

Of the 28 patients whose VEGF was measurable, there were 22 type A patients who expressed VEGF of 1827 ± 1697 ng/mg protein and 6 type B patients who expressed VEGF of 360 ± 184 ng/mg protein (Fig. 7). The amount of VEGF expression was significantly higher in the type A patients than in the type B patients ($P = 0.0138$).

Liver metastasis

The amount of VEGF expression in 7 patients whose tumor metastasized to the liver was 2818 ± 1979 ng/mg pro-

TABLE 1. Univariate Analysis Concerning the Relationship Between the Intratumoral Doppler Signal and Clinicopathological Characteristics

Factor	Type A	Type B	*P* Value
Age	64.7 ± 8.1	61.2 ± 8.8	0.1003
Gender			0.4052
Male	30	18	
Female	15	6	
Tumor location			0.4610
Head	20	13	
Body-tail	25	11	
Tumor size (cm)	4.0 ± 1.5	3.2 ± 1.3	0.0233*
CA19-9 (IU/mL)	8408 ± 22373	4243 ± 14419	0.3274
Hepatic metastasis			0.0052*
Positive	19	2	
Negative	26	22	
TNM categories			0.0216*†
T1, T2	5	9	
T3, T4	40	15	
			0.1153
N0	13	12	
N1	32	12	
			0.3116
M0	21	15	
M1	24	9	
Stage			0.0699
I, II	7	9	
III, IV	38	15	
Grade			0.8180
G1	6	3	
G2	16	10	
G3	10	4	

*Statistically significant.
†Fisher exact test.

TABLE 2. Multivariate Analysis of the Factors Associated With the Doppler Signal

Factor	Type A	Type B	r	95% Confidence Interval	*P* Value
Tumor size (cm)			0.00	0.180–1.722	0.3096
≥3.5	31	10			
<3.5	14	14			
Hepatic metastasis			−0.153	0.036–0.952	0.0435*
Positive	19	2			
Negative	26	22			
TNM			−0.100	0.088–1.187	0.0886
T1, T2	5	9			
T3, T4	40	15			

*Statistically significant.

tein, while that in the 18 patients who had no liver metastases was 1077 ± 1253 ng/mg protein, indicating a significant difference between the 2 groups ($P = 0.0241$).

DISCUSSION

According to immunohistochemical study of tumor vascularity, the number of intratumoral microvessel density (IMVD) in PC[4] is similar to that in gastric cancer and colon cancer.[29,30] However, compared with the pancreatic parenchyma, PC is imaged as an area of hypoattenuation[31–34] by dynamic CT and is positioned as a hypovascular tumor. While the microvessel density of nontumorous regions in the stomach and colon was slightly lower than that in the tumorous region, the microvessel density of normal pancreatic tissue was much higher than that in tumorous regions,[4] which is considered a major reason for hypovascular imaging of PC by dynamic CT. Even though there are reports of angiographically detected tumorous vascularization in 65% of cases,[35] it has been difficult to detect the intratumoral vessels in PC by conventional imaging.

As to the tumor vascularity detected by conventional Doppler ultrasonography, correlation with gastric cancer[36,37] and colon cancer[38] to IMVD was reported. Lassau et al[39,40] xenografted human colon tumor to mice and reported that Doppler signal corresponded with high vascular density (hot

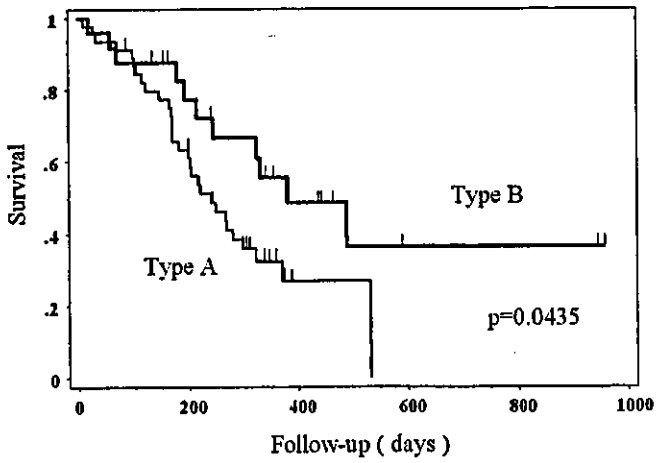

FIGURE 5. Patient survival time in relation to the vascular signal type. The mean survival duration of the type A group, which demonstrated vascular signals, was 283 ± 115 days, and that in the type B group, in which hardly any signal was detected, was 349 ± 241 days. The mean survival time of type A patients was significantly shorter than type B patients ($P = 0.0435$).

TABLE 3. Univariate Analysis Concerning the Relationship Between VEGF Expression and Clinicopathological Characteristics

Factor	n	VEGF ng/mg Protein	*P* Value
Doppler signal			0.0138*†
type A	22	1827 ± 1697	
Type B	6	360 ± 184	
Gender			0.7704†
Male	21	1595 ± 1748	
Female	7	1265 ± 1231	
Age	28		0.2110‡
Tumor size	28		0.7756‡
CA19-9	28		0.2534‡
Tumor location			0.1681†
Head	14	1070 ± 1229	
Body-tail	14	1955 ± 1874	
Hepatic metastasis			0.0241*†
Positive	7	2818 ± 1979	
Negative	21	1077 ± 1253	
TNM categories			0.1936†
T1, T2	3	447 ± 119	
T3, T4	25	1640 ± 1670	
			0.6472†
N0	8	1548 ± 1569	
N1	20	1499 ± 1679	
			0.3220†
M0	15	1277 ± 1435	
M1	13	1784 ± 1830	
Stage			0.7795†
I, II	6	1276 ± 1444	
III, IV	22	1577 ± 1689	
Grade			0.6692§
G1	1	3379	
G2	15	1411 ± 1593	
G3	8	1560 ± 2124	

*Statistically significant.
†Mann-Whitney *U* test.
‡Linear regression analysis.
§Kruskal-Wallis test.

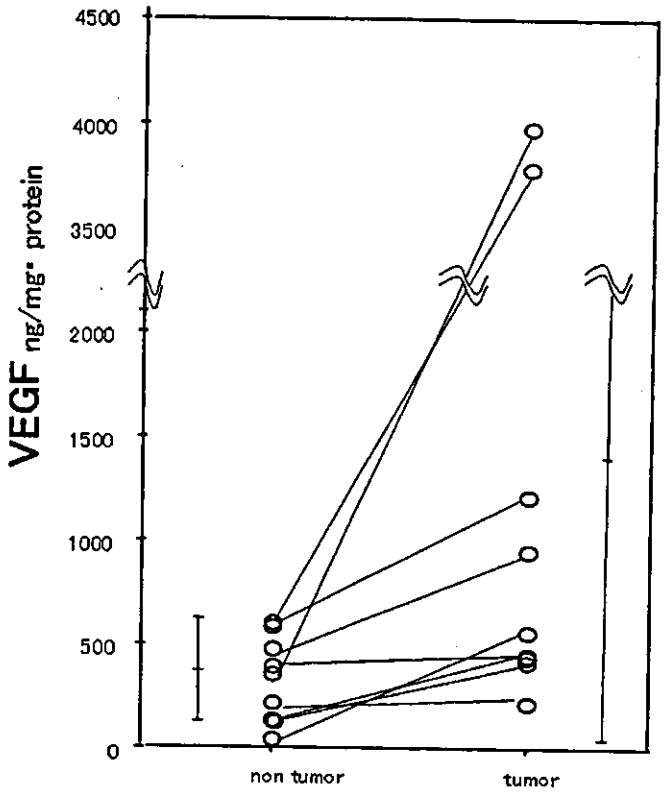

FIGURE 6. Comparison of amounts of VEGF expression in tumorous and nontumorous regions. The amounts of VEGF expression in nontumorous and tumorous regions were 408 ng/mg protein and 1469 ng/mg protein, respectively, indicating a significant difference between the 2 regions ($P = 0.0305$). The correspondence of the amount of VEGF expression in the tumorous region with that in the nontumorous region is shown by the connecting line in each case. Bar, mean ± SD.

spots) in tissue on color Doppler ultrasonography using Levosit and that tumorous vessels measuring 15 μm in minimal diameter were imaged. With regard to vascular flow in the pancreas revealed by ultrasonography, there have been some reports on imaging of peripheral arteries of the pancreas by the color Doppler method,[41,42] the contrast effect of ultrasonography by arterial injection of CO_2,[43,44] and the contrast effect of pulse inversion method[45] in the imaging of PC. There have been hardly any reports clearly describing imaging of intratumoral vessels in PC.[11] Compared with the conventional narrow-band Doppler method,[46,47] the dynamic flow method used in this study is highly sensitive and yields higher resolution and lower artifacts. The intratumoral vascular signals were imaged in about two-thirds of cases of PC by dynamic flow in this study. The ratio was much higher than that previously reported.[45]

Angiogenesis is essential for the proliferation and metastasis of tumors,[48] and VEGF is a major vascularization factor. In PC tissue, a trace volume of VEGF protein is observed in fibroblasts and a moderate volume in vascular smooth muscle cells, but VEGF protein is mainly expressed in the cytoplasm of tumor cells.[9,48] It is also reported that IMVD in PC, which is supposed to reflect newly formed tumor vessels, correlates with VEGF expression,[8,9,49] although VEGF does not correlate too strongly with the IMVD in nontumorous pancreatic tissue, which already have blood vessels. Furthermore, there have been reports on the correlation between IMVD in PC and liver metastasis[50] and between the level of VEGF ex-

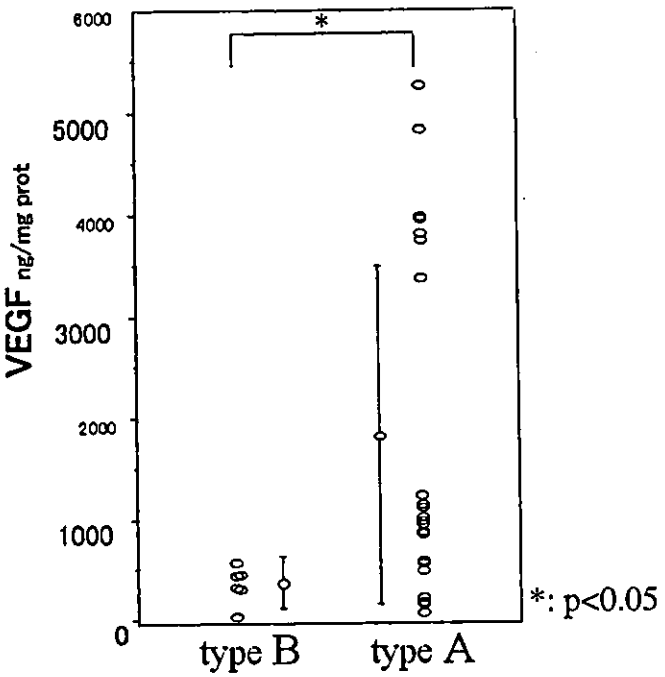

FIGURE 7. Relationship between vascular signal type detected by dynamic flow and amount of VEGF expression in the tumor tissue. The amount of VEGF expression in the type A group, which demonstrated vascular signals, was a mean of 1827 ng/mg protein and that in the type B group, in which hardly any signal was detected, was 360 ng/mg protein. The amount of VEGF expression in the type A group was significantly higher than that in the type B group ($P = 0.0138$). Bar, mean ± SD.

pression and patients' prognosis.[8] We quantitated VEGF protein in the tumorous tissue by EIA and evaluated the relationships among VEGF expression, vascular signal types, and clinical factors. The expression of VEGF protein was 3.6 times higher in tumorous tissue than in nontumorous tissue of the pancreas. Furthermore, the amount of VEGF expression in PC tissue was significantly higher in the patients with definite vascular signal as determined by dynamic flow and was also correlated with liver metastasis. In addition, multivariate analysis between the intensity of intratumoral vascular signals and the clinicopathological features showed that the patients with vascular signals had a significantly higher rate of liver metastasis and a higher degree of the T category. Although a correlation between color Doppler signal and distant metastasis after resection was reported in colon cancer,[38] this is the first report that describes the relationships between intratumoral blood flow detected by ultrasonography and clinicopathological characteristics including liver metastasis in PC.

The liver is the most common and critical site of metastasis affecting prognosis. The clinical parameters that predict liver metastasis have yet to be established. If these parameters are established and become available, they will be useful in improving prognostic stratification and designing future treatment strategies. The extent of tumor angiogenesis is reported to be a critical factor in determining the metastatic potential.[48] If imaging diagnosis can capture and image the vessels in PC, its results will be useful for predicting metastasis and prognosis. Using dynamic flow, it was possible to image the small vessels in the pancreas, although this had been difficult with conventional ultrasonography. Assessment of the intensity of intratumoral vascular signals by dynamic flow may become a noninvasive and easy method with which to predict liver metastasis.

We intend to accumulate more cases and investigate the clinical usefulness of dynamic flow.

ACKNOWLEDGMENT

We extend our gratitude to Dr. Tsutomu Komazawa, Professor Emeritus, and Prof. Yoshiyuki Sakamoto, The Institute of Statistical Mathematics, who assisted us in conducting the statistical analysis.

REFERENCES

1. Stuhrmann M, Aronius R, Schietzel M. Tumor vascularity of breast lesions: potentials and limits of contrast-enhanced Doppler sonography. *AJR Am J Roentgenol.* 2000;175:1585–1589.
2. Sedelaar MJP, Leenders GJLH, Kaa CAHD, et al. Microvessel density: correlation between contrast ultrasonography and histology of prostate cancer. *Eur Urol.* 2001;40:285–293.
3. Weidner N. Intratumor microvessel density as a prognostic factor in cancer. *Am J Pathol.* 1995;147:9–19.
4. Ellis LM, Takahashi Y, Fenoglio CJ, et al. Vessel counts and vascular endothelial growth factor expression in pancreatic adenocarcinoma. *Eur J Cancer.* 1998;34:337–340.
5. Cheng WF, Lee CN, Chu JS, et al. Vascularity index as a novel parameter for the in vivo assessment of angiogenesis in patients with cervical carcinoma. *Cancer.* 1999;85:651–657.
6. Takebayashi Y, Akiyama S, Yamada K, et al. Angiogenesis as an unfavorable prognostic factor in human colorectal carcinoma. *Cancer.* 1996; 78:226–231.
7. Linder S, Blåsjö M, Rosen A, et al. Pattern of distribution and prognostic value of angiogenesis in pancreatic duct carcinoma. *Pancreas.* 2001;22: 240–247.
8. Seo Y, Baba H, Fukuda T, et al. High expression of vascular endothelial growth factor is associated with liver metastasis and a poor prognosis for patients with ductal pancreatic adenocarcinoma. *Cancer.* 2000;88:2239–2245.
9. Itakura J, Ishiwata T, Friess H, et al. Enhanced expression of vascular endothelial growth factor in human pancreatic cancer correlates with local disease progression. *Clin Cancer Res.* 1997;3:1309–1316.
10. Yamanaka Y, Friess H, Buchler M, et al. Overexpression of acidic and basic fibroblast growth factors in human pancreatic cancer correlate with advanced tumor stage. *Cancer Res.* 1993;53:5289–5296.
11. Rickes S, Ocran K, Neye H, et al. Evaluierung dopplersonographischer Kriterien zur Differentialdiagnostik von Pankreastumoren. *Ultraschall Med.* 2000;21:253–258.
12. Schrope B, Newhouse VL, Uhlendorf V. Simulated capillary blood flow measurement using a nonlinear ultrasonic contrast agent. *Ultrason Imaging.* 1992;14:134–158.
13. Goldberg BB, Liu JB, Burns PN, et al. Galactose-based intravenous sonographic contrast agent: experimental studies. *J Ultrasound Med.* 1993;12: 463–470.
14. Calliada F, Campani R, Bottinelli O, et al. Ultrasound contrast agents: basic principles. *Eur J Radiol.* 1998;27:S157–S160.
15. Delorme S, Peschke P, Zuna I, et al. Sensitivity of color Doppler sonography: an experimental approach. *Ultrasound Med Biol.* 1999;25:541–547.

16. Petrick J, Zomack M, Schlief R. An investigation of the relationship between ultrasound echo enhancement and Doppler frequency shift using a pulsatile arterial flow phantom. *J Invest Radiol.* 1997;32:225–235.
17. Kono Y, Moriyasu F, Mine Y, et al. Gray scale second harmonic imaging of the liver with galactose-based microbubbles. *Invest Radiol.* 1997;32: 120–125.
18. Forsberg F, Goldberg BB, Liu JB, et al. On the feasibility of real time, in vivo harmonic imaging with proteinaceous microspheres. *J Ultrasound Med.* 1996;15:853–860.
19. Choi BI, Kim TK, Han JK, et al. Vascularity of hepatocellular carcinoma: assessment with contrast enhanced second-harmonic versus conventional power Doppler US. *Radiology.* 2000;214:381–386.
20. Kim TK, Han JK, Kim AY, et al. Limitations of characteristics of hepatic hemangiomas using a sonographic contrast agent (Levovist) and power Doppler ultrasonography. *J Ultrasound Med.* 1999;18:737–743.
21. Albrecht T, Hoffmann CW, Schettler S, et al. B-mode enhancement at phase-inversion US with air-based microbubble contrast agent: initial experience in humans. *Radiology.* 2000;216:273–278.
22. Burns PN, Wilson SR, Simpson DH. Pulse inversion imaging of liver blood flow: improved method for characterizing focal masses with microbubble contrast. *J Invest Radiol.* 2000;35:58–71.
23. Bauer A, Hauff P, Lazenby J, et al. Wideband harmonic imaging: a novel contrast ultrasound imaging technique. *Eur Radiol.* 1999;3(suppl): S364–S367.
24. Kim TK, Choi BI, Han JK, et al. Hepatic tumors: contrast agent-enhancement patterns with pulse inversion harmonic US. *Radiology.* 2000;216:411–417.
25. Koito K, Hirokawa N, Ichimura T, et al. Pancreatic tumors: diagnosis with contrast-enhanced sonography by using wide band Doppler technology. *Ultrasound Med Biol.* 2003;29(suppl 5):S165–166.
26. Sobin LH, Wittekind C, eds. *UICC TNM Classification of malignant tumours.* 5th ed. New York: John Wiley & Sons, 1997.
27. Köppel G, Solcia E, Longnecker DS, et al. *Histological typing of tumors of the exocrine pancreas. World Health Organization.* 2nd ed. Berlin: Springer-Verlag, 1996:15–21.
28. Kido S, Kitadai Y, Hattori N, et al. Interleukin8 and vascular endothelial growth factor—prognostic factors in human gastric carcinomas? *Eur J Cancer.* 2001;l37:1482–1487.
29. Tomisaki S, Ohno S, Ichiyoshi Y, et al. Microvessel quantification and its possible relation with liver metastasis in colorectal cancer. *Cancer.* 1996; 77(suppl 8):1722–1728.
30. Ueda T, Oda T, Kinoshita T, et al. Neovascularization in Pancreatic ductal adenocarcinoma: microvessel count analysis, comparison with noncancerous regions and other types of carcinomas. *Oncol Rep.* 2002;9:239–245.
31. Lu DSK, Vedantham S, Krasny RM, et al. Two-phase helical CT for pancreatic tumors: pancreatic versus hepatic phase enhancement of tumor, pancreas and vascular structures. *Radiology.* 1996;199:697–701.
32. Furukawa H, Takayasu K, Mukai K, et al. Late contrast-enhanced CT for small pancreatic carcinoma: delayed enhanced area on CT with histopathological correlation. *Hepatogastroenterology.* 1996;43:1230–1237.
33. Keogan MT, McDermottt VG, Paulson EK, et al. Pancreatic malignancy: effect of dual-phase helical CT in tumor detection and vascular opacification. *Radiology.* 1997;205:513–518.
34. Freeny PC, Marks WM, Ryan JA, et al. Pancreatic ductal adenocarcinoma: diagnosis and staging with dynamic CT. *Radiology.* 1988;166: 125–133.
35. Tylén U. Accuracy of angiography in the diagnosis of carcinoma of the pancreas. *Acta Radiol.* 1973;14:449–466.
36. Chen CN, Cheng YM, Lin MT, et al. Association of color Doppler vascularity index and microvessel density with survival in patients with gastric cancer. *Ann Surg.* 2002;235:512–518.
37. Kawasaki T, Ueo T, Itani T, et al. Vascularity of advanced gastric carcinoma: evaluation by using power Doppler imaging. *J Gastroenterol Hepatol.* 2001;16:149–153.
38. Chen CN, Cheng YM, Liang JT, et al. Color Doppler vascularity index can predict distant metastasis and survival in colon cancer patients. *Cancer Res.* 2000;60:2892–2897.
39. Lassau N, Paturel-asselin C, Guinebretiere JM, et al. New hemodynamic approach to angiogenesis: color and pulsed Doppler ultrasonography. *J Invest Radiol.* 1999;34:194–198.
40. Lassau N, Koscielny S, Opolon P, et al. Evaluation of contrast-enhanced color Doppler ultrasound for the quantification of angiogenesis in vivo. *J Invest Radiol.* 2001;36:50–55.
41. Uzawa M, Karasawa E, Sugiura N, et al. Doppler color flow imaging in the detection and quantitative measurement of the gastroduodenal artery blood flow. *J Clin Ultrasound.* 1993;21:9–17.
42. Tomiyama T, Ueno N, Tano S, et al. Assessment of arterial invasion in pancreatic cancer using color Doppler ultrasonography. *Am J Gastroenterol.* 1996;91:1410–1416.
43. Koito K, Namieno T, Nagakawa T, et al. Inflammatory pancreatic masses: differentiation from ductal carcinomas with contrast-enhanced sonography using carbon dioxide microbubbles. *AJR Am J Roentgenol.* 1997;169: 1263–1267.
44. Kato T, Tsukamoto Y, Naitoh Y, et al. Ultrasonographic and endoscopic ultrasonographic angiography in pancreatic mass lesions. *Acta Radiol.* 1995;36:381–387.
45. Oshikawa O, Tanaka S, Ioka T, et al. Dynamic sonography of pancreatic tumors: comparison with dynamic CT. *AJR Am J Roentgenol.* 2002;178: 1133–1137.
46. Kim AY, Choi BI, Kim TK, et al. Hepatocellular carcinoma: power Doppler US with a contrast agent—preliminary results. *Radiology.* 1998;209: 135–140.
47. Forsberg F, Liu JB, Burns PN, et al. Artifacts in ultrasonic contrast agent studies. *J Ultrasound Med.* 1994;13:357–365.
48. Folkman J. Angiogenesis in cancer, vascular, rheumatoid and other disease. *Nat Med.* 1995;1:27–31.
49. Fujioka S, Yoshida K, Yanagisawa S, et al. Angiogenesis in pancreatic carcinoma: thymidine phosphorylase expression in stromal cells and intratumoral microvessel density as independent predictors of overall and relapse-free survival. *Cancer.* 2001;92:1788–1797.
50. Teraoka H, Sawada T, Nishihara T, et al. Enhanced VEGF expression and decreased immunogenicity induced by TGF-beta1 promote liver metastasis of pancreatic cancer. *Br J Cancer.* 2001;85:612–617.

Diagnostic Imaging for Pancreatic Cancer

Computed Tomography, Magnetic Resonance Imaging, and Positron Emission Tomography

Hiromitsu Saisho, MD, and Taketo Yamaguchi, MD

Abstract: Computed tomography (CT), magnetic resonance imaging (MRI), and positron emission tomography (PET) are sophisticated modalities typically used in the second-line diagnosis following routine clinical practice. Among them, CT is regarded as the standard imaging in diagnosing pancreatic cancer at present in Japan due to its popularity and reasonable reliability in wide-ranging diagnostic ability. However, even with multidetector row CT (MDCT), the demonstration of pancreatic cancer less than 1 cm in size remains nearly impossible. CT staging is considered accurate in one-half to two-thirds of patients, but limitations in the imaging of peripancreatic microinvasion and nodal or hepatic micrometastases still have a tendency to underestimate tumor extension. With recent advancement in imaging techniques, MRI has proven to be equal or superior to other imaging modalities in diagnosing pancreatic cancer. Most of all, it is expected that MRCP will become as effective an instrument as ultrasonography (US) in the screening of pancreatic cancer. Functional imaging with PET using the glucose analog FDG can be used in the diagnosis of pancreatic cancer, but systemic or local disturbance of glucose metabolism may result in an incorrect diagnosis. The usefulness of PET is now considered in assessing tumor viability, monitoring tumor response to treatment, and detecting distant metastases.

Key Words: computed tomography, magnetic resonance imaging, positron emission tomography, magnetic resonance cholangiopancreatography, pancreatic carcinoma, clinical staging of pancreatic carcinoma

(*Pancreas* 2004;28:273–278)

In the diagnosis of pancreatic disease, computed tomography (CT), magnetic resonance imaging (MRI), and positron emission tomography (PET) are typically second-line procedures used to detect pancreatic lesions in patients who have experienced specific symptoms and/or undergone baseline studies, such as measurement of pancreatic enzymes and tumor markers, biochemistry, ultrasound examination, or other routine procedures. While CT and MRI are similar in diagnostic ability, CT use is more popular in the medical facilities of Japan due to its excellent space resolution and broad distribution of the machines. In the recent advent of multidetector row CT (MDCT), it is possible to generate more elaborate and informative images using the multiplanar reconstruction technique. Among MRI applications, MR cholangiopancreatography (MRCP) has become a favorable alternate to endoscopic retrograde cholangiopancreatography (ERCP) in the early diagnosis of pancreatic disease. Although the value of PET in the early detection of pancreatic carcinoma remains unclear, it does appear that PET is useful in the recognition of distant metastases and evaluation of therapeutic effects.

Received for publication November 4, 2003; accepted January 7, 2004.

From the Department of Medicine and Clinical Oncology, Graduate School of Medicine, Chiba University, Chiba, Japan.

Reprints: Hiromitsu Saisho, MD, 1-8-1, Inohana, Chuo-ku Chiba 260-0856, Japan (e-mail: saisho@faculty.chiba-u.jp).

COMPUTED TOMOGRAPHY

Despite the recent advent of various diagnostic modalities, dynamic CT (dual-phase contrast-enhanced CT) remains the most important procedure in the diagnosis of pancreatic carcinoma. CT can be used in almost all stages of the diagnostic process, from detection of the pancreatic carcinoma, to differentiation, to evaluation of tumor extension and staging.

Detection and Differentiation of Pancreatic Carcinoma Using Dynamic CT

For the dynamic study of the pancreas using single-detector helical CT, we used a power injector to employ 150 mL of 60% iodinated contrast material intravenously at a rate of 3 mL/s. Scanning began 40 seconds after the start of the injection, and overlapping sections throughout the pancreas were obtained at 5-mm intervals. Four to 5 minutes after the completion of contrast injection, the late-phase sections were obtained from the top of the liver through the pancreas, continuing at 1-cm intervals. With the conventional, single-detector CT machine, slice thickness is typically 1 cm for rapid data acquisition; with MDCT, it may be sharpened to 2 mm, which reasonably provides much more accurate images.

Invasive ductal carcinoma of the pancreas is hypovascular in character, and typical CT findings from the early phase of dynamic CT show a hypodensity mass less enhanced than the

remaining pancreas. In larger tumors, nonstaining areas frequently appear in the center of the mass and are thus recognized as the central necrosis. When associated with such nonstaining areas, the hypodensity mass is a more reliable indicator of ductal cancer. With these typical parameters, CT may facilitate correct diagnosis in more than 90% of pancreatic ductal carcinoma patients.[1] However, the features of contrast enhancement are variable, depending on the size of the tumor and the histologic variation of the carcinoma. Especially in respect to early diagnosis, it should be noted that the smaller the tumor, the less the characteristics of hypodensity are demonstrated.

In our series of 8 patients with small ductal carcinomas (≤2 cm in diameter), the tumors in 6 patients appeared as hypodensity masses in the early phase of dynamic CT (Fig. 1), but tumors in the remaining 2 patients were equally enhanced with the surrounding pancreas and were thus not indicated. Relatively intense enhancement of tumors in the late phase of dynamic CT was observed in 3 patients, including the 2 with previously unenhanced, early-phase tumors (Fig. 2).[2] Late-phase enhancement may be useful in the diagnosis of small carcinomas that are undetected in early-phase images. Nevertheless, the demonstration of carcinomas <1 cm in size may be almost impossible at present, even with MDCT.

Evaluation of Extension and Staging of Pancreatic Carcinoma Using Dynamic CT

Although the prognosis for patients with pancreatic carcinoma remains poor, survival may depend on the stage of the tumor at diagnosis and its resectability. According to current data from the Pancreatic Cancer Registration Committee of the Japan Pancreas Society (JPS), the 5-year survival rates of patients with invasive ductal carcinoma of the pancreas are 58.6%, 51.0%, 25.9%,11.9%, and 2.8% for patients with JPS stage I, II, III, IVa, and IVb tumors, respectively.[3]

While clinical judgment is important, reliable staging of tumors is crucial to select resectable candidates with reasonable expected survival and avoid unnecessary laparotomy. A pancreatic tumor is considered resectable when CT shows an isolated intrapancreatic mass, with or without bile duct or pancreatic duct dilatation. Tumors are considered unresectable if one or more of the following CT findings are present: local tumor extension beyond the gland, contiguous organ invasion, vascular involvement, nodal and/or liver metastases, or ascites. Based on these criteria, Freeny et al[1] concluded that in their series of 174 patients, CT had a 100% positive predictive value in the diagnosis of unresectable lesions; the negative predictive value in the diagnosis of resectable tumors was only 54%. Using thin-section CT, Fuhrman et al[4] gained promising results, showing that 37 (88%) of 42 patients considered by CT criteria to have resectable carcinomas of the pancreas underwent potentially curative resection. Nevertheless, the inaccurate preoperative assessment of resectability is based on the poor accuracy of CT imaging in detecting lymph node metastases, microscopic local tumor extension, and small hepatic metastases.

Diagnosis of lymph node metastases is considered to be the most important issue with respect to curable resection. The diagnostic accuracy of CT imaging of nodal metastases is reported to vary from 42% to 58%, the sensitivity from 19% to 37%, the specificity from 60% to 92%, the positive predictive value from 47% to 83%, and the negative predictive value from 34% to 67%.[5–10]

According to a recent study thoroughly conducted by Roche et al,[11] CT prospectively identified 40 lymph nodes from a total of 159 found in surgical specimens from 9 patients with pancreatic ductal adenocarcinoma. Of these 40 nodes, 7

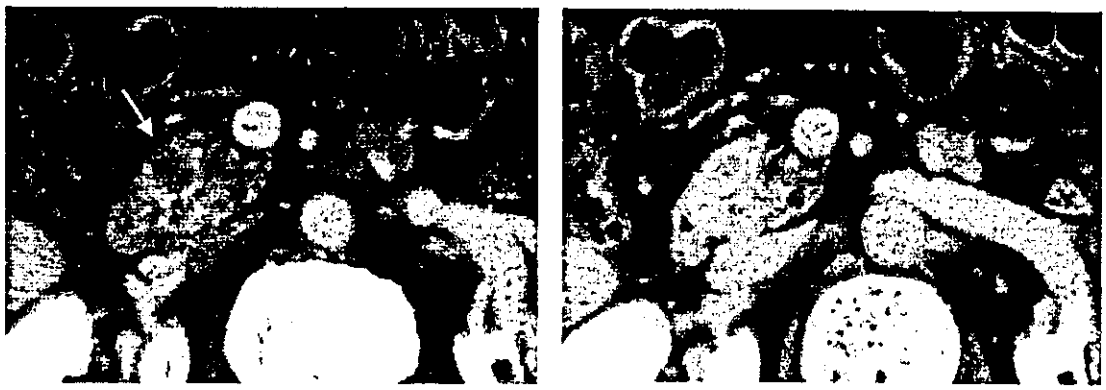

a b

FIGURE 1. A small pancreatic carcinoma displaying the typical pattern of the tumor in dynamic CT images. A: In the early phase, a hypodensity tumor (arrow) is shown to be hypovascular, compared with the contrast-enhanced parenchyma of the pancreas head. B: In the late phase, the tumor silhouette becomes unclear and even shows a spot of decreased attenuation remaining in the central area.

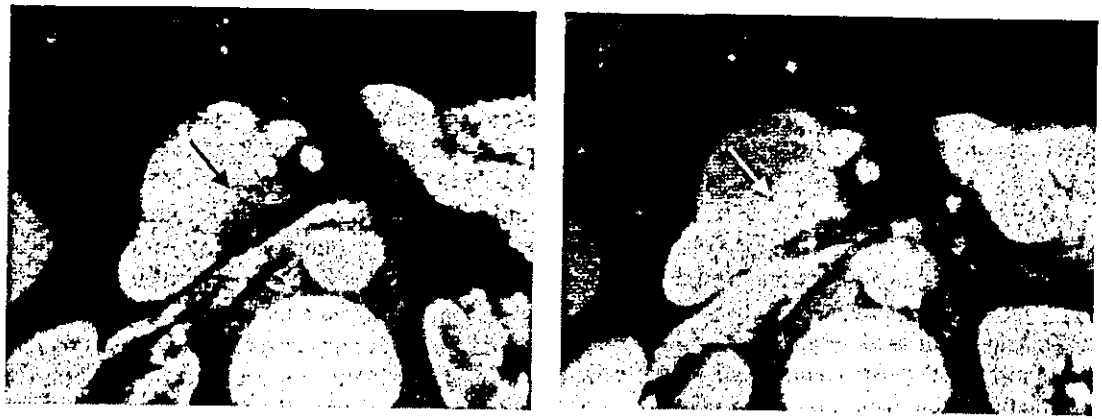

a b

FIGURE 2. A small pancreatic carcinoma is difficult to diagnose with CT. A: In the early phase of dynamic CT, an area of decreased attenuation (arrow) can be seen on the posterior surface of the pancreas head. B: In the late phase, intense attenuation due to contrast enhancement covers the same area.

were malignant, ie, the positive predictive value was 17%. Twenty-two of the remaining 119 nodes not identified by CT contained metastases; the negative predictive value was 81%. The sensitivity (detection rate of metastatic nodes), specificity, and overall accuracy were 24%, 75%, and 65%, respectively. When Roche et al focused on the 40 nodes shown on CT using a node size >5 mm as the criterion for involvement, they concluded that the sensitivity, specificity, and positive and negative predictive values were 71%, 64%, 29%, and 91%, respectively. With regard to the present report, it is surprising that the 6 nodes detected on CT that had short-axis diameters >10 mm included only 1 metastasis. Because we are not aware of specific indications for diagnosis other than tumor size, the question of CT accuracy must be considered. Further large-scale studies are anticipated.

In our own series of 35 patients with pancreatic carcinoma who underwent surgical resection, prospective diagnoses using CT were compared with the histopathological results from surgical specimens. The lymph nodes identified on CT were categorized using the JPS classification system, and each group was then correlated with a specific histopathology. The sensitivity of CT in detecting metastatic lymphadenopathy, with identified nodes >5 mm in diameter considered malignant, remained at a low value of 48.6% (18 of 37), but the positive predictive value of a diagnosis of involved nodes retained a reasonable reliability of 78.3% (18 of 23). For assessment of other factors of tumor extension, including involvement of the peripancreatic arteries, involvement of the portal vein system, anterior peripancreatic invasion, and posterior peripancreatic invasion, the results of CT accuracy were considered very reasonable in practice: 82.6%, 87.5%, 87.9%, and 71.9%, respectively. When assessed using the JPS system[12] and the UICC system,[13] the CT staging was accurate: 57% and 65%, respectively, with underestimation of 29% and 26% and overestimation of 14% and 9% (Fig. 3).

Thus, CT staging is considered accurate in one-half to two-thirds of patients, but limitations in the imaging of peripancreatic microinvasion and nodal or hepatic micrometastases still have a tendency to underestimate tumor extension. A high incidence of concurrent reactive lymphadenopathy with pancreatic carcinoma is another challenge that confronts CT staging of tumor extension. Future research is needed to explore and overcome these challenges, although at present, CT evaluation of the local extension and distant metastases proves to be indispensable in the management of patients with pancreatic carcinoma.

MAGNETIC RESONANCE IMAGING

MRI has not been as valuable a tool as CT in the diagnosis of pancreatic cancer due to the low resolution of MR and

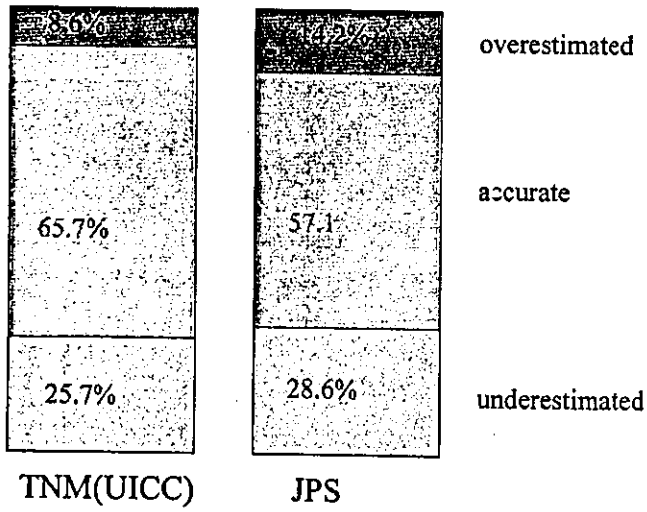

FIGURE 3. Accuracy of CT in the staging of pancreatic carcinoma, as evaluated in comparison with histologic staging in resected specimens from 35 patients.

the high number of artifacts produced with motion or respiration. However, recent technological advances in MRI have greatly improved its ability to visualize pancreatic cancer.[14–16] In addition, MRCP has been recently developed and is reported to be useful in the noninvasive demonstration of the morphologic contour of the pancreatic duct.[17]

MRI Protocol and Imaging of the Pancreas

Recent advancements in imaging techniques include T1-weighted, fat-suppressed imaging, contrast-enhanced dynamic studies, T2-weighted imaging with single-shot fast-spin echo (SSFSE or HASTE), and MRCP. Fast-scanning MR techniques have enabled breath-holding pancreatic imaging with fewer motion artifacts and have facilitated dynamic enhanced imaging during multiple phases of contrast enhancement.

With T1-weighted imaging, the normal pancreas displays relatively higher signal intensity than muscle or spleen, and surrounding fat tissue is delineated with high-signal intensity. T1-weighted, fat-suppressed imaging, on the other hand, produces low signal intensity from surrounding fat, which leads to a much higher intensity from the pancreatic parenchyma. Therefore, pancreatic cancer appears as a low signal intensity mass within the normal pancreatic parenchyma. However, this tissue contrast is not conspicuous, and contrast-enhanced dynamic studies are often required to obtain a clear image of the pancreatic cancer.

In contrast-enhanced dynamic studies, the normal pancreas displays strong enhancement during the arterial phase after rapid injection with gadolinium. Conversely, pancreatic cancer appears as a hypointensity mass similar to that on a dynamic CT scan.[18]

MR angiography and MR venography techniques using gadolinium contrast can demonstrate tumor invasion of major arteries or portal veins and preclude the need for conventional angiography.[19]

T2-weighted MRI may be limited in detecting pancreatic cancer because of insufficient T2 prolongation of the tumor. To this end, SSFSE (HASTE) is advantageous because it enables visualization of both biliary or pancreatic ducts and pancreatic parenchyma or the tumor.[12]

MRCP allows direct imaging of the pancreatic duct and does not require endoscopic procedure or irradiation nor is it associated with any complications. Images obtained by MRCP are highly comparable with those produced by ERCP and readily demonstrate pancreatic duct obstruction and dilatation.[20] Findings and diagnostic criteria for pancreatic cancer obtained using MRCP imaging are by no means different from those obtained with ERCP (Fig. 4).

Diagnostic Ability of MR in Imaging Pancreatic Cancer

Several studies have indicated that MRI is equal or superior to CT in the detection of pancreatic cancer. The tumor detection rate is reported to be 90%.[15,21] However, it is difficult to detect small or early-stage pancreatic cancer, and there is a lack of sophisticated reports concerning the diagnostic ability of MRI in detecting early pancreatic cancer. The role of MRI is thus considered to lie in the differential diagnosis and evaluation of tumor extension.

Differentiation between pancreatic cancer and chronic pancreatitis is often difficult, especially considering the focal enlargement of the so-called tumor-forming pancreatitis or inflammatory pancreatic mass. Dynamic MRI cannot successfully distinguish pancreatic cancer from chronic pancreatitis on the basis of degree and time of enhancement of the tumor.[22] On the other hand, a recent study reported an MRI accuracy rate of 91% in differentially diagnosing benign versus malignant pancreatic masses.[21] In another assessment, MRCP images revealed duct penetration, which is useful in the differen-

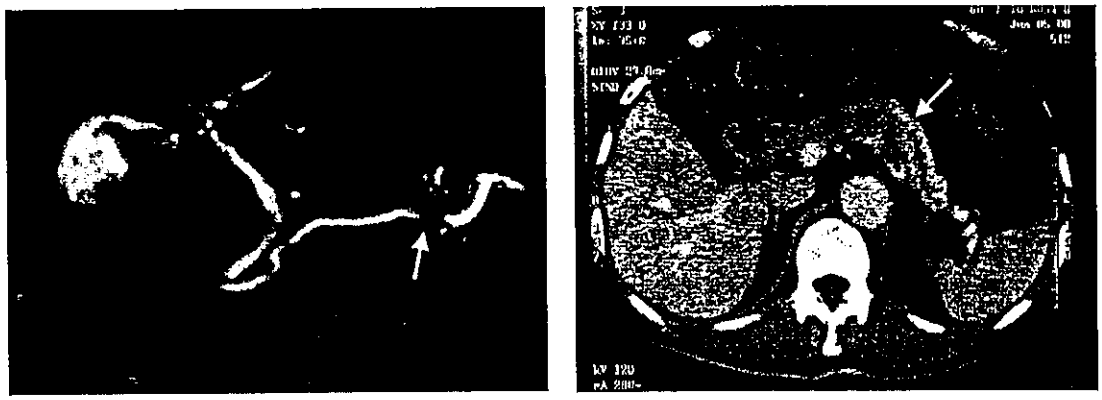

a b

FIGURE 4. Typical images of pancreatic carcinoma produced by MRCP and dynamic CT. A: MRCP image demonstrates the stenosis of the main duct in the pancreatic body. B: CT scan shows a small cancer <2 cm in diameter in the body of the gland that corresponds with the site of the stenosis shown in the MRCP image (arrow).

tiation of an inflammatory pancreatic mass from pancreatic cancer.[23]

Correct evaluation of tumor extension is crucial in determining a strategy for the treatment of pancreatic cancer. MRI is highly accurate in revealing vascular infiltration and liver metastasis, and a recent report gave diagnosis accuracy rates of approximately 90% for each.[20,24] In contrast, lymph node metastasis is difficult to detect, and accuracy of MRI is limited as is CT. Overall, the accuracy of MRI in detecting the nonresectability of a tumor is reportedly >90%, compared with CT and EUS.[24]

The majority of patients with pancreatic cancer have ductal stenosis or obstruction with dilatation of the proximal pancreatic duct, with or without dilatation of the bile duct. In a recent study, MRCP was found to be as sensitive as ERCP in detecting pancreatic cancer. In a prospective study measuring usefulness in diagnosing pancreatic cancer, MRCP and ERCP yielded equal rates of sensitivity and specificity (84%–91% and 63%–97% vs. 70%–94% and 50%–94%, respectively).[25,26] Sai and Ariyama[27] reported that 5 of 41 patients with tumors <2 cm in diameter with confirmed pancreatic cancer were successfully diagnosed using MRCP.

Practicality of MRI in the Early Diagnosis of Pancreatic Cancer

Although at many institutions, MRI is still only valued as supplementary to CT or ultrasonography (US), it has proven to be equal or superior to other imaging modalities in diagnosing pancreatic cancer, as mentioned above. One session of MR examination, in combination with T1-weighted fat-suppressed imaging, contrast-enhanced dynamic studies, MR angiography, and MRCP, may eliminate the need for CT, ERCP, and angiography. It is anticipated that MRCP will become as effective an instrument as US in the screening of pancreatic cancer.

POSITRON EMISSION TOMOGRAPHY

PET with ^{18}F-2-fluoro-2-deoxy-D-glucose (FDG) has emerged as a tool that can be used to diagnose pancreatic carcinoma. The basis of cancer detection using PET involves the increase in glucose metabolism by cancer cells. The glucose analog FDG is transported into tumor cells at a higher rate than normal tissues, accumulating in the tumor and allowing it to be imaged in contrast to surrounding tissue. This functional imaging is now applied in the diagnosis of various cancers.

PET can be used to facilitate detection of pancreatic carcinoma and to image its differentiation or characterization, staging, assessment of recurrence, and response to therapy. Various reports from the literature have shown that PET is very useful and accurate in the diagnosis of carcinoma of the pancreas. Zimny et al[28] evaluated PET accuracy in the diagnosis of pancreatic carcinoma in 106 patients with unclear pancreatic masses and obtained a sensitivity of 85%, a specificity of 84%, a positive predictive value of 93%, and a negative predictive value of 71%. However, the disturbance of glucose metabolism seen in diabetes mellitus, which is often associated with pancreatic carcinoma, is apt to reduce the sensitivity of PET,[29] and active inflammation caused by chronic pancreatitis may also result in a false-positive diagnosis of carcinoma.[30,31] The major drawback of PET is that it produces poor anatomic definition, and its usefulness in diagnosing pancreatic carcinomas of diameters of ≤2 cm remains unclear.

Nakamoto et al[32] reported a 90% accuracy of PET in detecting liver metastases from pancreatic carcinoma; 7 metastatic lesions indistinguishable from small cysts on US or CT were defined. However, a more conservative report stated the sensitivity of PET to be 54% for liver metastases and 61% for lymph node metastases.[33] Similar to other imaging modalities, PET's recognition of a tumor is limited by the amount of cancer cell mass that reflects the magnitude of FDG accumulation. Inflammatory lymphadenopathies may also diminish the accuracy of staging with PET.

Nevertheless, functional imaging with PET is considered useful in assessing tumor viability and monitoring tumor response to treatment. Because PET has the ability to image the entire body in 1 setting, it is not surprising that it is also useful in the detection of distant metastases that spread outside the scope of CT or other imaging techniques.

REFERENCES

1. Freeny PC, Marks WM, Ryan J, et al. Pancreatic ductal adenocarcinoma: diagnosis and staging with dynamic CT. *Radiology*. 1988;166:125–133.
2. Matsuura N, Saisho H, Yamaguchi T, et al. Clinical study on the efficacy of contrast enhanced CT scan for the diagnosis of pancreatic cancer: with special reference to the evaluation of new CT findings useful for differentiation from tumor forming pancreatitis [in Japanese]. *Chiba Igaku*. 1995;71:141–149.
3. Pancreatic Cancer Registration Committee in Japan Pancreas Society. Pancreatic cancer registration of JPS: the summary for 20 years [in Japanese]. *J Jpn Pancreas Soc*. 2003;18:101–169.
4. Fuhrman GM, Charnsangavej C, Abbruzzese JL, et al. Thin-section contrast-enhanced computed tomography accurately predicts the resectability of malignant pancreatic neoplasms. *Am J Surg*. 1994;167:104–113.
5. Megibow AJ, Zhou XH, Rotterdam H, et al. Pancreatic adenocarcinoma: CT versus MR imaging in the evaluation of resectability—report of the radiology diagnostic oncology group. *Radiology*. 1995;195:327–332.
6. Midwinter MJ, Beveridhe CJ, Wilsdon JB, et al. Correlation between spiral computed tomography, endoscopic ultrasonography and findings at operation in pancreatic and ampullary tumours. *Br J Surg*. 1999;86:189–193.
7. Palazzo L, Roseau G, Gayet B, et al. Endoscopic ultrasonography in the diagnosis and staging of pancreatic adenocarcinoma: results of a prospective study with comparison to ultrasonography and CT scan. *Endoscopy*. 1993;25:143–150.
8. Zeman RK, Cooper C, Zeiberg AS, et al. TNM staging of pancreatic carcinoma using helical CT. *AJR Am J Roentgenol*. 1997;169:459–464.
9. Roesch T, Braig C, Gain T, et al. Staging of pancreatic and ampullary carcinoma by endoscopic ultrasonography: comparison with conventional sonography, computed tomography, and angiography. *Gastroenterology*. 1992;102:188–199.
10. Mueller MF, Meyenberger C, Bertschinger P, et al. Pancreatic tumors: evaluation with endoscopic US, CT, and MRI imaging. *Radiology*. 1994; 190:745–751.
11. Roche CJ. Hughes ML, Garvey CJ, et al. CT and pathologic assessment of

prospective nodal staging in patients with ductal adenocarcinoma of the head of the pancreas. *AJR Am J Roentgenol.* 2003;180:475–480.
12. Japan Pancreas Society. *General rules for the study of pancreatic cancer* [in Japanese], 4th ed. Tokyo: Kanehara-Shuppan; 1993.
13. International Union Against Cancer (UICC). *TNM classification of malignant tumours*, 5th ed. New York: John Wiley & Sons; 1997.
14. Semelka RC, Ascher SM. MR imaging of the pancreas. *Radiology.* 1993; 188:593–602.
15. Ichikawa T, Haradome H, Hachiya J, et al. Pancreatic ductal adenocarcinoma: preoperative assessment with helical CT versus dynamic MR imaging. *Radiology.* 1997;202:655–662.
16. Ito K, Koike S, Matsunaga N. MR imaging of pancreatic diseases. *Eur J Radiol.* 2001;38:78–93.
17. Barish MA. Sato JA. MR cholangiopancreatography: techniques and clinical applications. *AJR Am J Roentgenol.* 1997;169:1295–1303.
18. Gabata T, Matsui O, Kadoya M, et al. Small pancreatic adenocarcinoma: efficacy of MR imaging with fat suppression and gadolinium enhancement. *Radiology.* 1994;193:683–688.
19. Shirkhoda A, Konez O, Shetty A. Mesenteric circulation: three-dimensional MR angiography with gadolinium-enhanced multiecho gradient-echo technique. *Radiology.* 1997;169:1295–1303.
20. Barish MA, Yucel EK, Ferruch JT. Magnetic resonance cholangiopancreatography. *N Engl J Med.* 1999;341:258–264.
21. Hanninen EL. Amthauer H, Hosten N, et al. Prospective evaluation of pancreatic tumors: accuracy of MR imaging with MR cholangiopancreatography and MR angiography. *Radiology.* 2002;224:34–41.
22. Johnson PT, Outwater EK. Pancreatic carcinoma versus chronic pancreatitis: dynamic MR imaging. *Radiology.* 1999;212:213–218.
23. Ichikawa T, Sou H, Araki T, et al. Duct-penetrating sign at MRCP: usefulness for differentiating inflammatory pancreatic mass from pancreatic carcinomas. *Radiology.* 2001;221:107–116.
24. Schima W, Fugger R, Schober E, et al. Diagnosis and staging of pancreatic cancer: comparison of mangafodipir trisodium- enhanced MR imaging and contrast-enhanced helical hydro-CT. *AJR Am J Roentgenol.* 2002; 179:717–724.
25. Albert JG. ERCP and MRCP—when and why. *Best Pract Res Clin Gastroenterol.* 2002;16:399–419.
26. Calvo MM, Bujanda L, Calderon A, et al. Comparison between magnetic resonance cholangiopancreatography and ERCP for evaluation of the pancreatic duct. *Am J Gastroenterol.* 2002;97:347–353.
27. Sai J, Ariyama J. Imaging diagnosis of pancreatic cancer: MRI (MRCP) [in Japanese]. *Consensus Cancer Ther.* 2003;2:16–19.
28. Zimny M, Bares R, Fass J, et al. Fluorine-18 fluorodeoxyglucose positron emission tomography in the differential diagnosis of pancreatic carcinoma: a report of 106 cases. *Eur J Nucl Med.* 1997;24:678–682.
29. Diederichs CG, Staib L, Glatting G, et al. FDG PET: elevated plasma glucose reduces both uptake and detection rate of pancreatic malignancies. *J NuclMed.* 1998;39:1030–1033.
30. Shreve PD. Focal fluorine-18 fluorodeoxyglucose accumulation in inflammatory pancreatic disease. *Eur J Nucl Med.* 1998;25:259–264.
31. Nakamoto Y, Saga T, Ishimori T, et al. FDG-PET of autoimmune-related pancreatitis: preliminary results. *Eur J Nucl Med.* 2000;27:1835–1838.
32. Nakamoto Y, Higashi T, Sakahara H, et al. Contribution of PET in the detection of liver metastases from pancreatic tumours. *Clin Radiol.* 1999; 54:248–252.
33. Bares R, Dohmen BM, Cremerius U, et al. Results of positron emission tomography with fluorine-18 labeled fluorodeoxyglucose in differential diagnosis and staging of pancreatic carcinoma. *Radiologe.* 1996;36:435–440.

Contrast-Enhanced Sonography of Autoimmune Pancreatitis

Comparison With Pathologic Findings

Kazushi Numata, MD, Yutaka Ozawa, MD, Noritoshi Kobayashi, MD, Toru Kubota, MD, Nozawa Akinori, MD, Yukio Nakatani, MD, Kazuya Sugimori, MD, Toshio Imada, MD, Katsuaki Tanaka, MD

Objective. We evaluated the vascularity of autoimmune pancreatitis lesions on contrast-enhanced harmonic gray scale sonographic images in comparison with the pathologic findings. ***Methods.*** Six patients with autoimmune pancreatitis were examined. All patients held their breath from 20 to 50 seconds after the injection of a contrast agent while the vascularity of the lesion was examined by contrast-enhanced harmonic gray scale sonography (early phase), and lesion enhancement was monitored at about 90 seconds after the injection while the patients held their breath for a few seconds (delayed phase). We then compared the vascularity on the contrast-enhanced harmonic gray scale sonographic images with the pathologic findings (fibrosis and inflammation) in all lesions. The vascularity of 3 of the 6 lesions was also evaluated by contrast-enhanced harmonic gray scale sonography before and after treatment with corticosteroids. ***Results.*** The autoimmune pancreatitis lesions exhibited mild (n = 1), moderate (n = 3), or marked (n = 2) enhancement throughout almost the entire lesions in both the early and delayed phases. The grade of lesion vascularity on the contrast-enhanced harmonic gray scale sonographic images correlated with the pathologic grade of inflammation and inversely correlated with the grade of fibrosis associated with autoimmune pancreatitis. The vascularity of all 3 lesions had decreased on the contrast-enhanced harmonic gray scale sonographic images after steroid therapy. ***Conclusions.*** Contrast-enhanced harmonic gray scale sonography may be useful for evaluating the vascularity of autoimmune pancreatitis lesions and the therapeutic efficacy of steroid therapy. ***Key words:*** autoimmune pancreatitis; contrast-enhanced sonography; pathologic findings.

Abbreviations
CT, computed tomography

Received June 10, 2003, from the Gastroenterological Center (K.N., K.S., T.I., K.T.) and Department of Pathology (N.A., Y.N.), Yokohama City University Medical Center, Yokohama, Japan; and Third Department of Internal Medicine (Y.O., N.K.) and Second Department of Surgery (T.K.), Yokohama City University School of Medicine, Yokohama, Japan. Revision requested July 10, 2003. Revised manuscript accepted for publication October 1, 2003.

We thank Kanae Saito, Yoshiro Haruna, Yoshiro Okaya, Zuhua Mao, and Simm Christoph from Siemens Medical Solutions for providing technical advice and Manabu Morimoto, Kazuhito Shirato, and Osamu Kunihiro from the Gastroenterological Center, Yokohama City University Medical Center, for providing additional assistance.

Address correspondence and reprint requests to Kazushi Numata, MD, Gastroenterological Center, Yokohama City University Medical Center, 4-57 Urafune-cho, Minami-ku, Yokohama 232-0024, Japan.

E-mail: kz-numa@zero.ad.jp.

Autoimmune pancreatitis is a rare type of chronic pancreatitis and is characterized by enlargement of all or part of the pancreas, irregular narrowing of the main pancreatic duct, hyperglobulinemia, the presence of autoantibodies, and a marked response to steroid therapy.[1-6] In the initial stage of autoimmune pancreatitis, the glands in the pancreatic head are almost always enlarged to a greater degree than in the body and tail,[7] and histologic examination reveals fibrotic change with lymphocyte infiltration.[2] Both the irregular narrowing of the main pancreatic duct and distal bile duct stricture improve in varying degrees in response to steroid therapy.[7]

Contrast-enhanced harmonic gray scale sonography has recently been used to evaluate the vascularity of pancreatic mass lesions,[8,9] and it allows visualization of blood perfusion in pancreatic mass lesions without motion artifacts.[9] It is also a very simple, noninvasive procedure that can be performed on an outpatient basis and can be used in patients in renal failure and in patients who are allergic to iodine contrast agents. We have reported that contrast-

enhanced harmonic gray scale sonography can be used to distinguish pancreatic carcinomas from focal inflammatory mass lesions or hypervascular pancreatic tumors[9]; however, there have been no reports on evaluation of autoimmune pancreatitis by contrast-enhanced gray scale sonography. In this study, we used contrast-enhanced harmonic gray scale sonography to evaluate the vascularity of pancreatic lesions in autoimmune pancreatitis and then compared the results with the pathologic findings.

Materials and Methods

Patients

Between January 2000 and July 2002, 6 patients with autoimmune pancreatitis were admitted to our institutions and examined by both helical computed tomography (CT) and contrast-enhanced harmonic gray scale sonography. Five of the 6 patients had jaundice caused by a sonographically visualized mass in the pancreatic head, and a pancreatic mass lesion and slight dilatation of the common bile duct detected on sonography were the initial findings in the other patient. The mean ± SD maximal diameter of the 6 pancreatic mass lesions was 36 ± 5 mm. All the patients had previously been examined by conventional sonography. All were male, and their ages ranged from 45 to 73 years (mean, 60 years).

The diagnosis of autoimmune pancreatitis was confirmed by histopathologic examination in all patients. Two patients had marked jaundice, and percutaneous transhepatic choledochal drainage was performed. Resection was performed in both patients because of the difficulty in differentiating between autoimmune pancreatitis and pancreatic carcinoma. Autoimmune pancreatitis lesions were suspected in the other 4 cases, and the diagnosis was made by open biopsy (n = 1) or aspiration biopsy (n = 3). The aspiration biopsies were performed with a 21-gauge fine needle (Sonopsy; Hakko, Tokyo, Japan) under conventional sonographic guidance. Informed consent was obtained from all patients.

Contrast-Enhanced Harmonic Gray Scale Sonography

Contrast-enhanced gray scale sonography was performed in all cases with a Sonoline Elegra system (Siemens Medical Solutions, Issaquah, WA) and a 3.5-MHz convex probe. The pancreas was scanned by native tissue harmonic gray scale imaging (transmit, 1.6, 1.8, or 2.0 MHz; receive, 3.2, 3.6, or 4.0 MHz, respectively). Then the pancreatic lesion was scanned by contrast-enhanced wideband phase inversion harmonic gray scale sonography (transmit, 2.5 or 2.8 MHz; receive, 5.0 or 5.6 MHz) at a frame rate of 1 to 5 frames/s, just before and after intravenous injection of a 300-mg/mL concentration of a galactose-palmitic acid contrast agent (Levovist [SH U 508A]; Schering AG, Berlin, Germany). Transmission power was 100%, and the mechanical index values were between 1.0 and 1.9. The focus position was just below the bottom of the lesion. Because a certain amount of time is probably required to completely fill pancreatic lesions with the sonographic contrast agent, especially in the setting of extensive fibrosis, we decided to evaluate lesion enhancement in 2 phases (early and delayed) of contrast-enhanced wideband harmonic gray scale sonography.[9] A 7-mL dose of Levovist was bolus injected at 0.5 mL/s via a 22-gauge cannula in an antecubital vein, and 5% glucose was continuously infused at 5.0 mL/min after the bolus injection of Levovist. The patients gently inhaled and then held their breath for about 30 seconds (starting between 20 and 50 seconds after the contrast medium injection) while the lesion was examined for enhancement (early phase). After observation of the early phase, we froze the image. The images were then reviewed frame-by-frame from cine loop memories and stored on magneto-optical disks. This procedure took approximately 15 to 35 seconds (mean, 25 seconds), and the time was used to allow pooling of the contrast agent within the pancreatic mass lesion. The entire lesion was then scanned and examined for enhancement at about 90 seconds after injection of the contrast agent while the patients held their breath for a few seconds (delayed phase). The images were frozen again and reviewed on a frame-by-frame basis with a cine loop and stored on a magneto-optical disk for hard copy printing. The entire examination was recorded on S-VHS videotape.

We graded enhancement of pancreatic mass lesions as "marked enhancement," "moderate enhancement," "mild enhancement," and "no contrast enhancement," compared with the pre-enhanced appearance on contrast-enhanced wideband phase inversion harmonic gray scale sonography. Marked enhancement was defined as enhancement during the early and delayed phases that was much greater than before infu-

sion of Levovist (Figure 1), mild enhancement as enhancement during the early and delayed phases that was slightly greater than before infusion of Levovist (Figure 2), moderate enhancement as enhancement during the early and delayed phases that was between mild and marked enhancement (Figure 3), and no contrast enhancement as enhancement during the early and delayed phases that was the same as before infusion of Levovist.

Helical CT

Helical CT with a Proceed SE system (GE Medical Systems, Milwaukee, WI) was performed in all patients. A dual-phase study was performed in each patient as follows. First, an unenhanced helical sequence through the pancreas and liver was obtained. Next, 100 mL of iohexol (Omnipaque; Sanofi Winthrop Pharmaceuticals, New York, NY) was infused into an antecubital vein at a rate of 3 mL/s; an

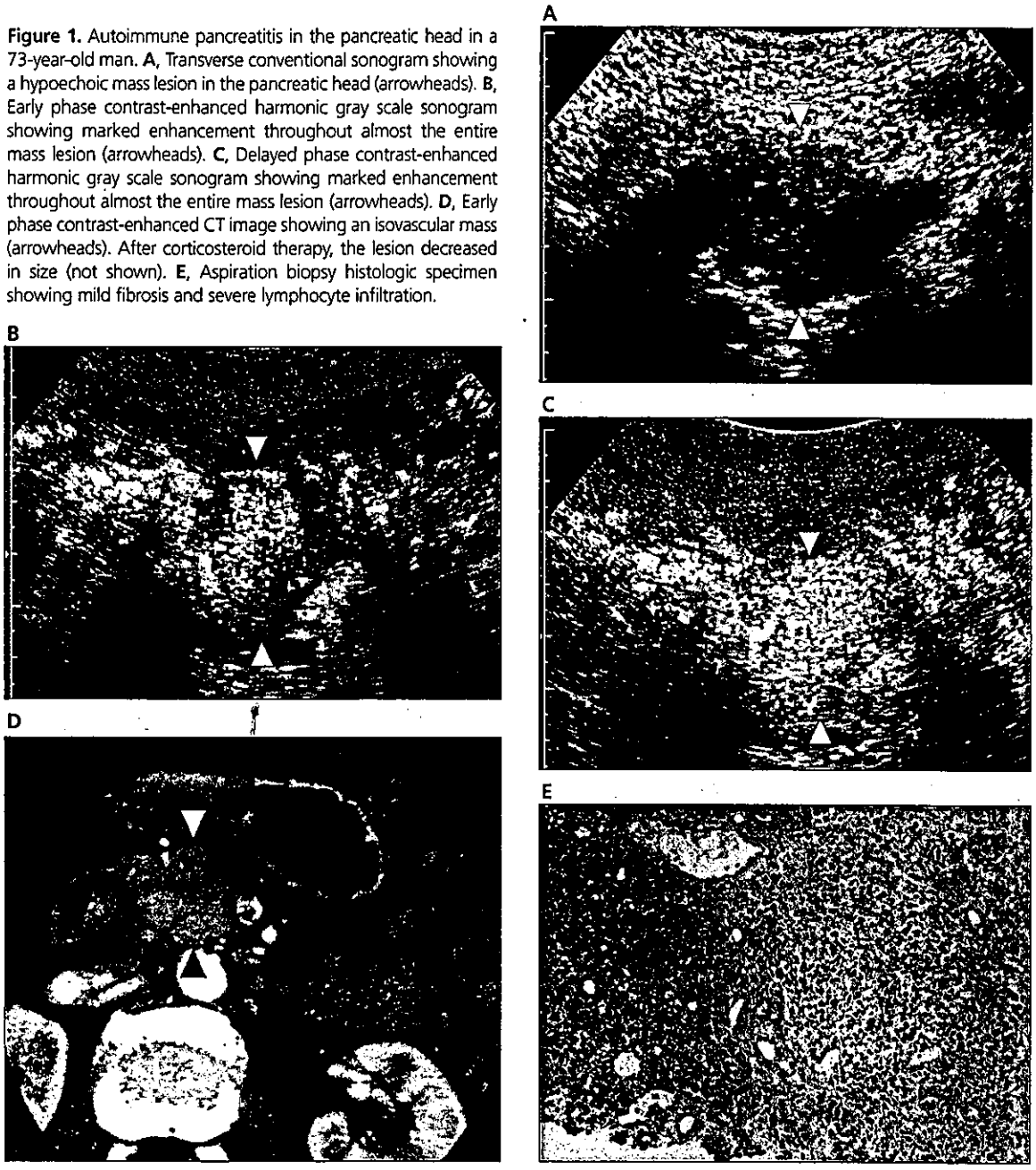

Figure 1. Autoimmune pancreatitis in the pancreatic head in a 73-year-old man. **A**, Transverse conventional sonogram showing a hypoechoic mass lesion in the pancreatic head (arrowheads). **B**, Early phase contrast-enhanced harmonic gray scale sonogram showing marked enhancement throughout almost the entire mass lesion (arrowheads). **C**, Delayed phase contrast-enhanced harmonic gray scale sonogram showing marked enhancement throughout almost the entire mass lesion (arrowheads). **D**, Early phase contrast-enhanced CT image showing an isovascular mass (arrowheads). After corticosteroid therapy, the lesion decreased in size (not shown). **E**, Aspiration biopsy histologic specimen showing mild fibrosis and severe lymphocyte infiltration.

early phase sequence was obtained after a delay of 25 sec; and a delayed phase sequence was obtained beginning 80 sec after the start of the infusion. All images were obtained in the helical mode with 5- or 7-mm collimation and a 5- or 7-mm/s table feed speed. Images were reconstructed at 5- or 7-mm intervals. The vascularity of mass lesions was graded as "hypervascular," "isovascular," and "hypovascular." Lesions were classified as hypervascular if they appeared denser than the surrounding pancreas during the early and delayed phases, isovascular if they appeared to have the same density as the surrounding pancreas during the early and delayed phases, and hypovascular if they appeared to be less dense than the surrounding pancreas during the early and delayed phases.

Pathologic Findings

Two pathologists who did not know the results of the contrast-enhanced harmonic gray scale sonography and helical CT studies evaluated the lesions for grade of fibrosis and inflammation. Fibrosis of the mass lesions was graded as "severe," "moderate," and "mild" on the basis of the severity of the fibrotic changes, and inflammation was graded as severe, moderate, and mild according to the severity of lymphocyte infiltration.

Steroid Therapy

Three patients were treated with prednisolone. The initial dose was 30 mg/d for 2 weeks and was then reduced 5 mg every 2 weeks. We performed contrast-enhanced harmonic gray scale sonog-

Figure 2. Autoimmune pancreatitis in the pancreatic head in a 60-year-old-man. **A,** Transverse early phase contrast-enhanced harmonic gray scale sonogram showing mild enhancement throughout almost the entire mass lesion (arrowheads). **B,** Delayed phase contrast-enhanced harmonic gray scale sonogram showing mild enhancement throughout almost the entire mass lesion (arrowheads). **C,** Early phase contrast-enhanced CT image showing an isovascular mass (arrowheads). **D,** Open biopsy histologic specimen showing severe fibrosis and mild lymphocyte infiltration.

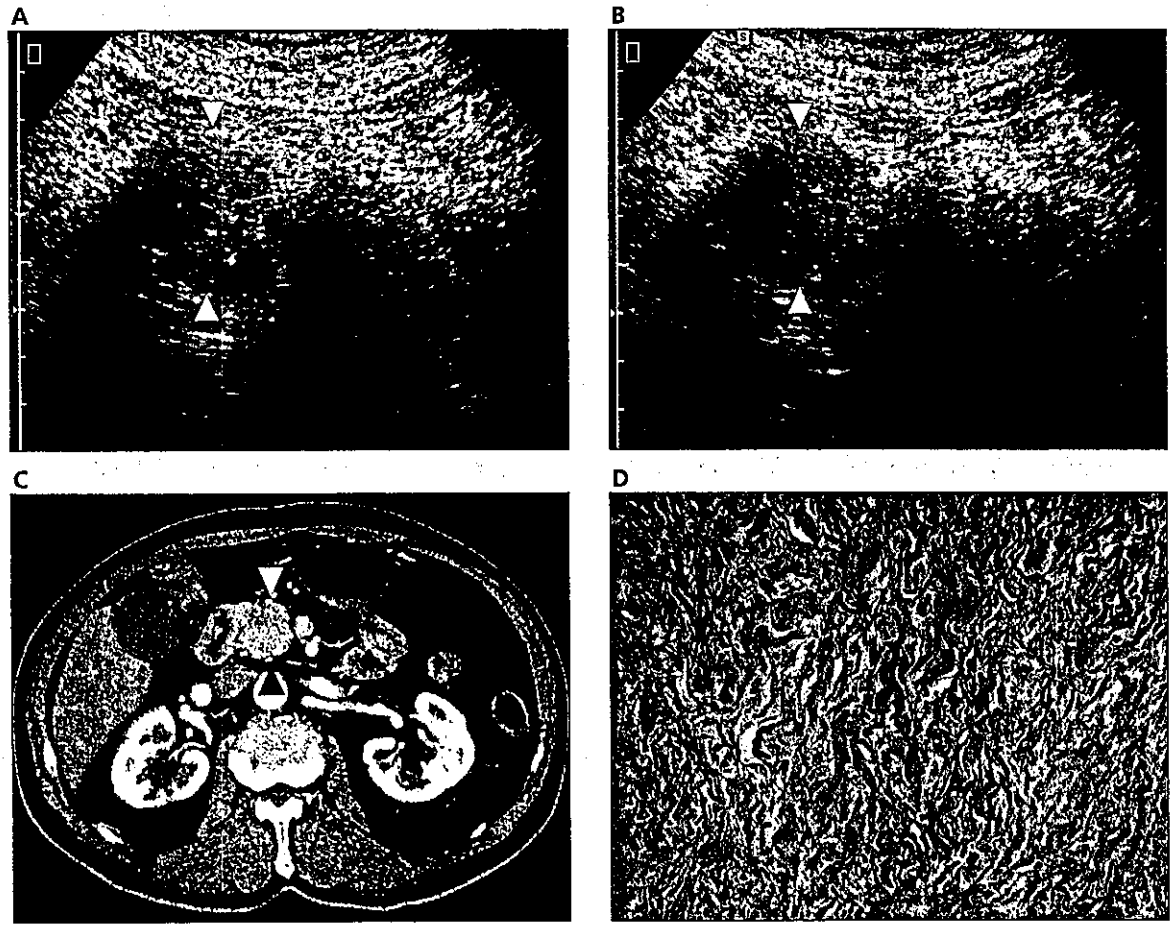

raphy 4 weeks after the start of steroid therapy and at the end of the steroid therapy to confirm the effectiveness of this therapy.

Image Analysis

The helical CT findings and contrast-enhanced harmonic gray scale sonographic findings were reviewed in a blinded fashion during 3 separate sessions at least 1 week apart. The evaluations were made by 4 of the authors (2 radiologists and 2 sonographers), who were unaware of the other study results. The studies were viewed in 3 different random orders to further eliminate the possibility of reviewer bias. Results were tabulated, and positive findings were compared at a consensus conference. Because 1 of the 6 lesions was classified differently by 2 authors, all 4 image evaluators met to arrive at a consensus for the final evaluation.

Statistical Analysis

Data are expressed as means ± SD.

Results

Comparison Between Contrast-Enhanced Harmonic Gray Scale Sonographic Findings and Helical CT Findings

All pancreatic lesions were initially detected on sonography. All patients with autoimmune pancreatitis were found to have dilatation of the common bile duct but no dilatation of the main pancreatic duct. No involvement of peripancreatic vessels was observed in any of the cases.

Figure 3. Autoimmune pancreatitis in the pancreatic head in a 45-year-old-man. **A**, Transverse early phase contrast-enhanced harmonic gray scale sonogram obtained before steroid therapy showing moderate enhancement throughout almost the entire mass lesion (arrowheads). **B**, Transverse early phase contrast-enhanced harmonic gray scale sonogram obtained 4 weeks after the start of steroid therapy showing mild enhancement throughout almost the entire mass lesion (arrowheads). The mass lesion is clearly decreased in size compared with the mass in **A**. An aspiration biopsy histologic specimen showed moderate fibrosis and moderate lymphocyte infiltration (not shown). **C**, Delayed phase contrast-enhanced CT image before steroid therapy showing an isovascular mass lesion (arrowheads). **D**, Delayed phase contrast-enhanced CT image 4 weeks after the start of steroid therapy showing an isovascular mass lesion (arrowheads). The lesion is clearly decreased in size compared with the mass in **C**.